Atlas55+: Brain Functional Atlas of Resting-state Networks for Late Adulthood

Gaelle E. Doucet[1,2,*], Loïc Labache[3], Paul M. Thompson[4], Marc Joliot[3], Sophia Frangou[1,5]

Abstract The human brain is intrinsically organized into resting-state networks (RSNs). Currently, several human brain functional atlases are used to define the spatial constituents of these RSNs. However, the only brain functional atlases available are derived from samples of adults under the age of 40 years. As brain networks are continuously reconfigured throughout life, the lack of brain atlases derived from older populations may influence results related to the RSN properties in late adulthood. To address this, here we aimed to construct a reliable brain atlas derived from older healthy participants only. To do so, we analyzed the resting-state functional magnetic resonance imaging data from three large independent cohorts of healthy individuals in late life (total N=563; age range: 55-95 years) and a mid-life cohort (total N=322; age range: 18-54 years). Using a multi-step independent component analysis approach, we identified five major RSNs (default mode, salience, executive control, sensorimotor, and visual networks) across all the individuals in each cohort. We demonstrated: (a) high spatial reproducibility across the three late-life cohorts with an average spatial overlap of 67%, with the salience network having the lowest score (46%) and the visual network having the highest score (83%); and (b) RSNs derived from the late-life cohorts were spatially different from those derived from the mid-life cohort (p=0.016). In response, we constructed a novel brain functional atlas, called Atlas55+, which includes a consensus of the major RSNs across the three late-life cohorts. We show that the RSNs of Atlas55+: (1) did not show detectable differences between males and females, (2) showed spatial differences from those identified in younger healthy individuals, and (3) were independent of variation in neuroimaging parameters and sample composition. Atlas55+ provides the first reliable age-appropriate template for the major RSNs in late adulthood and is publicly available. Our results confirm the need to construct age-appropriate brain functional atlases for studies investigating brain mechanisms related to aging.

Keywords Brain functional atlas · late adulthood · resting-state networks · aging

Corresponding author: (*)
Dr. Gaelle Doucet
Brain Architecture, Imaging and Cognition Lab
Boys Town National Research Hospital
555 N 30th street
Omaha, NE 68131
USA
gaelle.doucet@boystown.org
+1 (531) 355-6703

[1] Department of Psychiatry, Icahn School of Medicine at Mount Sinai, New York, NY, USA

[2] Boys Town National Research Hospital, Omaha, NE, USA

[3] GIN, UMR5293, CEA, CNRS, Bordeaux University, Bordeaux, France

[4] Imaging Genetics Center, Mark and Mary Stevens Neuroimaging and Informatics Institute, Keck School of Medicine, University of Southern California, Marina del Rey, CA, USA

[5] Centre for Brain Health, University of British Columbia, Vancouver, BC, Canada

Introduction

Resting-state functional magnetic resonance imaging (rs-fMRI) has been instrumental in mapping the brain functional connectome in health (Doucet et al., 2011; Fox et al., 2005; Smith et al., 2009; Smith et al., 2015) and disease (Buckner et al., 2009; Dong et al., 2018; Doucet et al., 2017; Feltz and Miller, 1996; Sha et al., 2019; Tracy and Doucet, 2015). The brain functional connectome can be defined as a multi-scale partition in which regions may be aggregated into networks, which in turn may be combined into larger systems (Abou Elseoud et al., 2011; Doucet et al., 2011; Kiviniemi et al., 2009). However, our previous work and others have suggested that the intermediate partition of the brain at the level of networks may be optimal to explain cognitive activity and to identify reliable biomarkers of neuropsychiatric and neurological disorders (Abou Elseoud et al., 2011; Doucet et al., 2011; Doucet et al., 2012; Doucet et al., 2017; Salman et al., 2019; van den Heuvel and Hulshoff Pol, 2010), while limiting the issue of multiple comparisons when compared to finer brain partitions (Zalesky et al., 2010). At this level of brain organization, five major resting-state networks (RSNs) have been typically identified across rs-fMRI studies: those involved in internally guided, higher order mental

functions as part of the intrinsic system (default-mode [DMN], executive control [ECN], and salience [SAL] networks) and those supporting externally driven, specialized sensory and motor processing as part of the extrinsic system (visual [VIS] and sensorimotor [SMN] networks) (Buckner et al., 2013; De Luca et al., 2006; Doucet et al., 2011; Doucet et al., 2019; Smith et al., 2009). Each of these brain networks relies on established white matter pathways (Greicius et al., 2009; Toosy et al., 2004; van den Heuvel et al., 2009) and has been consistently and robustly defined by their spatiotemporal configuration and functional roles (Damoiseaux et al., 2006; Doucet et al., 2011; Doucet et al., 2019; Elliott et al., 2019; Smith et al., 2009; van den Heuvel and Hulshoff Pol, 2010).

Several brain functional atlases are currently available which support reproducibility by harmonizing the RSN definition across neuroimaging studies (Doucet et al., 2019). However, to date, the only brain functional atlases available are derived from samples of young healthy adults, typically below the age of 40 years (Doucet et al., 2019). Nonetheless, changes in brain function over the course of adulthood have been well-documented and suggest that brain networks are continuously reconfigured throughout adult life (Betzel et al., 2014; Damoiseaux, 2017; Damoiseaux et al., 2008; He et al., 2013; Luo et al., 2020b; Meunier et al., 2009; Varangis et al., 2019b; Yaple et al., 2019). To our knowledge, there is currently no reference brain functional atlas derived from rs-fMRI data from older adults, and this may undermine neuroimaging efforts to characterize the brain functional connectome and its cognitive role in late adulthood. Critically, robust differences in the spatial composition of the RSNs derived from large samples of younger versus older adults have yet to be systematically investigated.

In this context, the current study focused on the spatial definition of the five major RSNs (DMN, ECN, SAL, VIS and SMN) in healthy adults aged 55 years and older. The specific aims were: (a) to test the reproducibility of the major RSNs in three large independent cohorts comprising a total of 563 healthy adults (age range: 55-95 years). We analyzed data from the Center for Ageing and Neuroscience (CamCAN) project (Shafto et al., 2014; Taylor et al., 2017), the Southwest University Adult Lifespan Dataset (SALD) (Wei et al., 2018) and the Alzheimer's Disease Neuroimaging Initiative (ADNI) database (Jack et al., 2008; Petersen et al., 2010); (b) to identify differences in the anatomical constitution of RSNs defined in the above cohorts compared to those in mid-life adults; and (c) generate a reliable consensual RSN atlas to enhance the reproducibility of template-defined RSNs in older adults.

Material and Methods

Cohorts

Late-life Cohorts: We used data from the CamCAN project (Shafto et al., 2014; Taylor et al., 2017), the SALD (Wei et al., 2018) and the ADNI database (Jack et al., 2008; Petersen et al., 2010). In each cohort, we selected healthy individuals aged 55 years and above for whom both rs-fMRI and structural MRI data were available. This selection resulted in a sample of 250 individuals for CamCAN (referred to as "CamCAN55+"), 190 for SALD and 134 for ADNI (details in supplementary material). Following quality control of the imaging data (described below), 11 participants across cohorts were removed for excessive head motion. The total analysis sample for the older individuals comprised 563 individuals, described in Table 1 and Supplementary Figure S1.

Mid-life Cohort: As the CamCAN cohort includes younger adults, a subset of this cohort, referred to "CamCAN55-", was also used to test for differences between younger and older adults in RSN spatial composition. The CamCAN55- included 326 individuals. Following the same quality control process, we excluded four individuals from CamCan55- (Table 1).

Resting-state fMRI Acquisition and Preprocessing

Acquisition parameters for the rs-fMRI data in each cohort are detailed in the Supplementary Material. Regardless of the cohort, the rs-fMRI data were preprocessed in an identical fashion, using SPM12 and the DPABI Toolbox (Yan et al., 2016).

Table 1. Cohort Characteristics. CamCAN: Cambridge Center for Ageing and Neuroscience, SALD: Southwest University Adult Lifespan Dataset, ADNI: Alzheimer's Disease Neuroimaging Initiative, TR: Repetition Time, rs-fMRI: Resting-state functional magnetic resonance imaging sequence.
* number of volumes vary by ADNI site, see detail in supplementary material.

Cohort	N	Age, years (Mean (SD))	Age Range (years)	Sex (% Females)	rs-fMRI TR (sec)	rs-fMRI Volumes	rs-fMRI Instruction
CamCAN55+	246	71.3 (9.3)	55-88	49%	1.97	261	closed eyes
SALD	185	63.1 (6.5)	55-80	61%	2.00	242	closed eyes
ADNI	132	78.9 (7.0)	62-95	50%	3.00	140-200*	open eyes
CamCAN55-	322	38.2 (9.7)	18-54	53%	1.97	261	closed eyes

Preprocessing procedures for the rs-fMRI datasets included removal of the first 3 volumes, motion correction to the first volume with rigid-body alignment; co-registration between the functional scans and the anatomical T1-weighted scan; spatial normalization of the functional images into Montreal Neurological Institute (MNI) stereotaxic standard space; spatial smoothing within the functional mask with a 6-mm at full-width at half-maximum Gaussian kernel; wavelet despiking (Patel et al., 2014); linear detrending; and regression of motion parameters and their derivatives (24-parameter model) (Friston et al., 1996), as well as white matter (WM), CSF time series. The WM and CSF signals were computed using a component based noise reduction method (CompCor, 5 principal components) (Behzadi et al., 2007). Lastly, bandpass filtering was applied at [0.01-0.1] Hz (Cordes et al., 2001).

As previously mentioned, across the three late-life cohorts, we excluded 11 individuals who had excessive head movement based on maximum transient (volume-to-volume) head motion above 2 mm translation or 1 degree rotation. After removing these individuals, we ensured that head motion, based on the mean framewise displacement (Power et al., 2012) did not correlate with age (r=0.08). Following the same process, we excluded 4 individuals from the CamCan55- cohort.

Resting-state Networks in the late-life cohorts

Resting-state networks identification in the late-life cohorts

We aimed to identify reliable brain networks using a process validated by Naveau et al. (2012). First, for each individual within each cohort, single-subject independent component analyses (ICAs) were conducted 20 times with random initialization using the Multivariate Exploratory Linear Optimized Decomposition into Independent Components (MELODIC) software, version 3.15, included in the FMRIB Software Library (FSL) v6.0.3 (http://www.fmrib.ox.ac.uk/fsl) (Smith et al., 2004). The number of independent components (ICs) was estimated by Laplace approximation (Minka, 2000). A symmetric approach of the FastICA algorithm (Hyvarinen, 1999) was used to compute the ICAs. Second, for each repetition, we used the multi-scale clustering of individual component algorithm (MICCA) to classify ICs into *N* groups (Naveau et al., 2012). The number of groups was automatically estimated by the algorithm (Naveau et al., 2012). Third, the Icasso algorithm (Himberg et al., 2004) was used to select the groups of reproducible ICs (i.e., groups with ICs that were present in at least 50% of the 20 repetitions), which we identified as the “group-level components” (Salman et al., 2019). Fourth, for each group-level component, a voxel-wise t-score map of individual ICs was computed and thresholded using a mixture model (p>0.95, (Beckmann and Smith, 2004)). Lastly, we discarded the group-level components if their spatial map: (i) mainly covered non-gray matter (i.e., CSF and WM), or (ii) included regions with strong signal attenuation due to susceptibility artefacts (i.e., lower frontal and lower temporal regions) (Supplementary Figures S2-S4).

Spatial Overlap of group-level components in late-life cohorts

Within each cohort, we mapped the spatial overlap across the group-level components by computing an index that quantified the number of group-level components overlapping at each voxel. This voxel-wise index ranged from 1 (no spatial overlap, the voxel is assigned to only one component) to *n* (where n is the maximum number of components overlapping at a voxel).

As the goal of the current study was to create a reliable functional atlas of RSNs, we created non-overlapping group-level components, on which we based the remaining analyses. To do this, each brain voxel was assigned to the group-level components with the highest *t*-score.

Reliability analyses of the group-level components in late-life cohorts

As the spatial configuration of a brain network is strongly related with its functional connectivity (Bijsterbosch et al., 2018), we conducted supplementary analyses to assess the functional reliability of each group-level component, in each cohort, following the methods described in Labache et al. (2020) (Supplementary Figure S5). In each cohort, we generated a dendrogram based on the average connectivity matrix between the group-level components. The functional reliability of a group-level component depended on the number of times it maintained the same position in the dendrogram of each individual participant of the same cohort. We created a reliability index (Q) for each group-level component, where a score close to zero indicated perfect functional reliability and a high score indicated high functional unreliability (details in supplementary information and supplementary Figure S5). We conducted Tukey’s fences tests to identify and discard these highly unreliable group-level components.

Construction of the major RSNs in late-life cohorts

We chose to focus on the major RSNs defined as: the DMN, the ECN, the SAL, the SMN, and the VIS (Doucet et al., 2011; Doucet et al., 2019; Smith et al., 2009) and examined their spatial definition across the three cohorts.

Following the identification of non-overlapping and functionally reliable group-level components in

each cohort, we proceeded to assigning them to the major RSNs of interest, namely the DMN, ECN, SAL, VIS and SMN. As reference for each network, we used their spatial definition in the Consensual Atlas of REsting-state Networks (CAREN) (Doucet et al., 2019). This atlas was generated by our group and presents the spatial configuration of the major RSNs based on their common properties across the most widely used brain functional atlases and as such it represents the most reproducible spatial features of the major RSNs currently available. This choice was also based on the fact that, to the best of our knowledge, there are currently no validated and reproducible RSNs from rs-fMRI data of a large sample of older healthy individuals, that we could use as normative templates.

In each cohort, we computed the Dice coefficient (Dice, 1945) to quantify the degree of spatial overlap between each group-level component and each of the five aforementioned CAREN RSNs. Components were then assigned to the RSN with which they had the largest overlap. We applied this process to each cohort separately to create spatial maps of the major RSNs. We were thus able to construct a spatial map for each RSN. We used the Dice coefficient to test the pairwise similarity between the same-labeled RSNs across cohorts. Lastly, to ensure that the results did not depend on the template used (i.e., CAREN), we also used the atlas created by Yeo et al. (2011) for the RSN assignment.

Spatial comparison of the major RSNs in late- and mid-life adults

To test for differences in the spatial constitution of RSNs in late- compared to mid-life adults, we applied the same procedure as for the late-life cohorts, to construct the major RSNs in CamCAN55- (Supplementary Figure S11).

We then compared their respective RSNs to those derived from the other two independent cohorts (ADNI and SALD). For this, we used Dice's coefficient to quantify the spatial similarity of the RSNs in CamCAN55-, and in CamCAN55+ respectively, to those of SALD and ADNI, and compared these pairwise coefficients (i.e., we compared the coefficients resulting from the RSN comparison CamCAN55+ vs. SALD and ADNI to those resulting from the mRSN comparison CamCAN55- vs. SALD and ADNI). This choice of approach was based on two major reasons: (1) among the three cohorts, CamCAN was the largest and also provided more reliable data (having the largest number of rs-fMRI volumes (Elliott et al., 2019), Table 1); and (2) this approach enabled us to account for differences in analytic approach, site, and MRI acquisition parameters.

Generation of Atlas55+

The major RSNs identified in each of the three late-life cohorts were used as input data to create a consensual 5-network atlas, named Atlas55+. For this, we used the function *consensus_similarity.m* from the Network Community Toolbox (http://commdetect.weebly.com), which constructs a representative partition.

To test the spatial reproducibility of Atlas55+, we conducted supplementary analyses: (1) we assigned each brain voxel to a network only if at least two of the three late-life cohorts assigned this voxel to the same network. We then computed a spatial correlation between the two versions of Atlas55+ using Pearson's correlation analyses. (2) We created a voxel-wise confidence map to quantify the consistency of the network assignment between the RSNs of the atlas and those from each of the 3 late-life cohorts. This voxel-wise index ranged from 0 (poor confidence, the network assignment of a voxel in Atlas55+ differed from its network assignment in all three cohorts) to 100% (high confidence, the network assignment of a voxel in Atlas55+ was identical to its network assignment in all three cohorts). Lastly, we compared the RSNs of the atlas to those of CamCAN55- in order to quantify the spatial differences between RSNs from younger adults and older adults, computing Dice coefficients.

To identify the anatomical definition of each RSN in the atlas, we generated subject-specific versions using a dual regression approach in FSL (Beckmann et al., 2009; Nickerson et al., 2017). We then entered each network into a one-sample *t* test, adding age, head motion (mean framewise displacement), estimated total intracranial volume (TIV, measured using FreeSurfer v6.0 (http://surfer.nmr.mgh.harvard.edu/), and site as covariates of no interest. Significant regions were reported at a $p<0.05$ after applying a family wise error (FWE) correction at the voxel level ($T>5.3$, cluster size>20 voxels).

Effects of sex and age on the RSNs in the Atlas55+

The effect of age on the spatial distribution of each RSN in the atlas (extracted from the dual regression) across all individuals (total $n=563$) was tested by conducting an analysis of covariance (ANCOVA), adding covariates of no interest: head motion, TIV, and site. Sex differences in the spatial distribution of the RSNs in the atlas were also assessed using age, head motion, TIV, and site as covariates of no interest. Significant clusters are reported at a $p<0.05$ with FWE correction at the voxel level ($T>5.3$, cluster size>20 voxels).

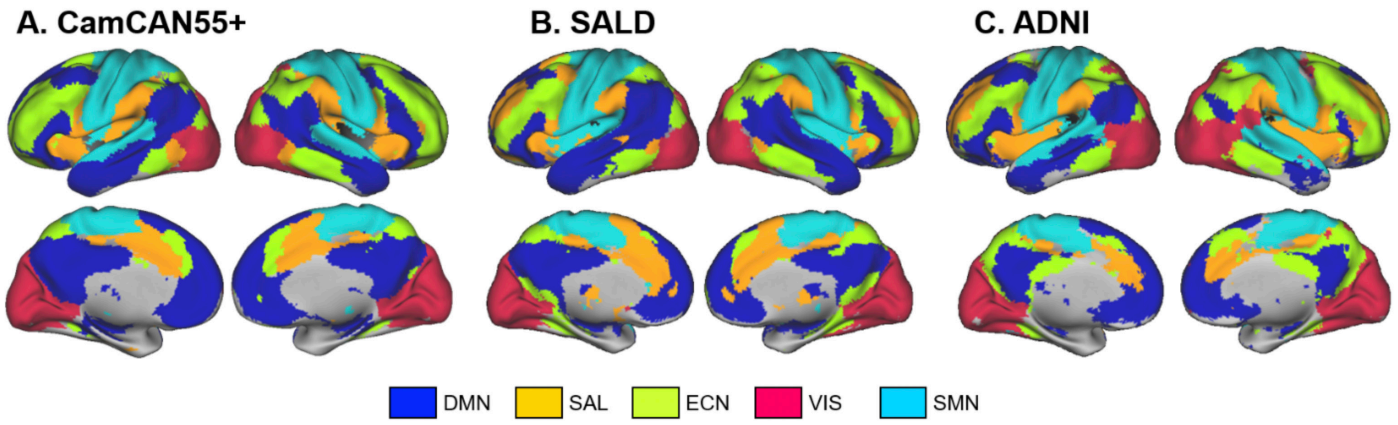

Figure 1. Spatial map of the five major RSNs. (A) CamCAN55+, (B) SALD, (C) ADNI. DMN: Default mode network, SAL: Salience network, ECN: Executive control network, VIS: Visual network, SMN: Sensorimotor network.

Results

Identification of group-level components in the late-life cohorts

In the CamCAN55+, SALD and ADNI cohorts, we respectively identified a total of 27, 24 and 23 reproducible group-level components (Supplementary Figures S2-S4 and S8). For the CamCAN55+ cohort, we found that 27% of the voxels were assigned to a single group-level component, while less than 0.5% of the voxels were assigned to a maximum of nine group-level components. The degree of spatial overlap between components was similar for the other two cohorts (Supplementary Figure S7). Regardless of cohort, the regions with the highest overlap were located in the medial posterior cortex, the dorso-medial prefrontal cortex and the lateral parietal cortex (Supplementary Figure S7).

Regardless of cohort, the functional reliability tests showed that all group-level components had a similar degree of stability, with no outlier, across individuals and in each cohort (Supplementary Figure S6). The reliability Q scores of each component did not differ across cohorts (p>0.1).

Construction and Reliability of the major RSNs in the late-life cohorts

The five RSNs constructed in each late-life cohort (Figure 1) showed high spatial reproducibility across the three cohorts with an average spatial overlap of 67% (mean range: 66-69%), with the SAL having the lowest score (46%) and the VIS having the highest score (83%) (Figure 2A). Supplementary Figure S9 shows the voxelwise confidence values with respect to the probability of a voxel being assigned to the same-labeled RSN across the three cohorts. The majority of voxels (83.5%) had confidence values over 66%, indicating that at least two out of the three cohorts had the same RSN assignment.

The choice of a reference atlas, CAREN or Yeo, minimally affected the spatial definition of the RSNs. The average spatial overlap of each RSN constructed based on CAREN versus each RSN constructed based on Yeo's atlas was 86% across the three cohorts (CamCAN: 86% (sd=15%), SALD: 85% (19%), ADNI: 86% (9%)) (Supplementary Figure S10).

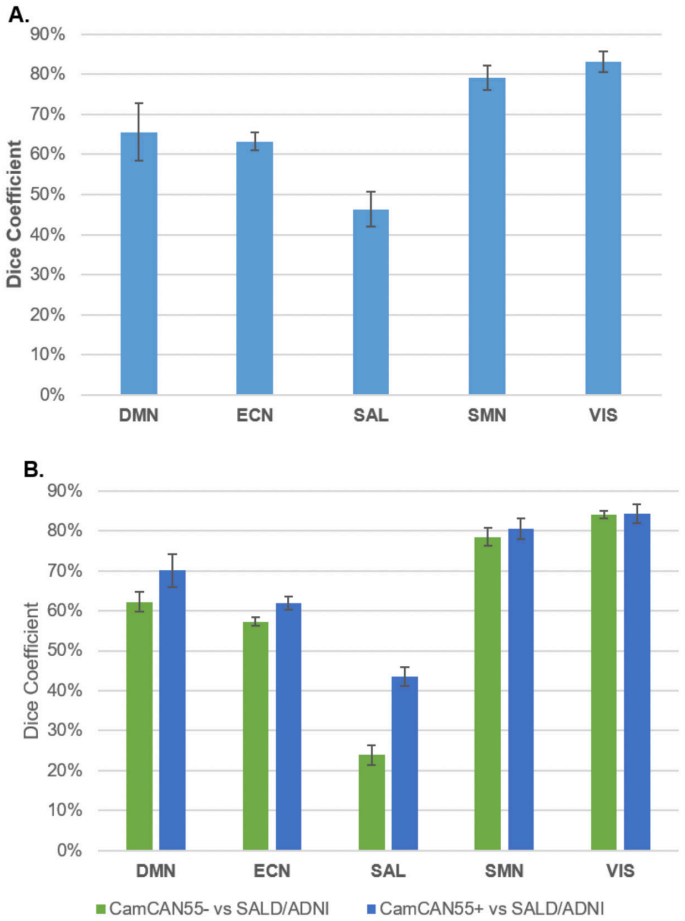

Figure 2. Spatial similarity of the RSNs across the cohorts. (A) Spatial similarity of the RSNs across the late-life cohorts. (B) Comparison of the spatial similarity of the RSNs identified in the CamCAN55- vs. the ADNI and SALD cohorts and in the CamCAN55+ vs. the ADNI and SALD cohorts. DMN: Default mode network, SAL: Salience network, ECN: Executive control network, VIS: Visual network, SMN: Sensorimotor network.

Comparison of the major RSNs between late- and mid-life adults

We found that the major RSNs in the CamCAN55- (Supplementary Figure S11) were less similar to those in the SALD and ADNI than the networks in the CamCAN55+ were (t=-3.0, p=0.016; Figure 2B). The SMN and VIS, which cover primary cortices differed the least, while the SAL was the network showing the largest spatial difference between the younger and older cohorts.

Atlas 55+

Atlas55+ includes the five major RSNs (DMN, ECN, SAL, SMN and VIS), based on the consensus of the three late-life cohorts (Figure 3A). The anatomical description of each network is detailed in Supplementary Table S2. The degree of confidence in network assignment in Atlas55+ was high across the three late-life cohorts (Figure 3B). The SMN and VIS were the most reproducible networks with 77% and 93% of their voxels consistently assigned across all three cohorts, respectively. They also showed the largest spatial overlap with their respective networks as outlined in CamCAN55- (spatial overlap: 76% and 85% respectively) (Figure 4). As defined in Atlas55+, the SMN was comprised of the sensory and motor regions (precentral and postcentral gyrus and supplementary motor area), the primary auditory cortex (superior temporal cortex), and thalamus while the VIS network largely covered the occipital lobe. For the DMN, 51% of the network's voxels showed consistency across all three cohorts. In Atlas55+, the DMN comprised the medial prefrontal cortex/ventral anterior cingulate cortex (ACC), the precuneus/posterior cingulate cortex (PCC), the inferior frontal cortex, the angular gyri, the middle temporal cortex, the hippocampi and amygdala, and some bilateral cerebellar clusters. It showed a 65% overlap with the DMN as defined in CamCAN55- (Figure 4). The major spatial differences were localized in the medial temporal lobe -which was part of the DMN from CamCAN55-, but not from Atlas55+ (Figure 4). For the ECN, 58% of the network's voxels showed consistency across all three cohorts. In Atlas55+, the ECN included parts of the dorsolateral prefrontal cortex, the lateral and medial parietal cortex, the posterior inferior temporal cortex, the posterior parahippocampal gyrus and some bilateral cerebellar clusters. It showed a 58% overlap with the ECN as defined in CamCAN55-. The major differences showed the recruitment of the posterior medial temporal lobe (lingual and parahippocampal gyri) in the ECN from Atlas55+. The SAL network emerged as the least reproducible network: 25% of the network's voxels were consistently assigned to the SAL across the three cohorts. In Atlas55+, the SAL was comprised of the anterior insula bilaterally, the dorsal ACC, the supramarginal gyri, subcortical regions including the putamen and thalamic nuclei, and bilateral cerebellar clusters. The spatial overlap with the SAL defined in CamCAN55- was the lowest with 21% and the regional differences were widespread (Figure 4).

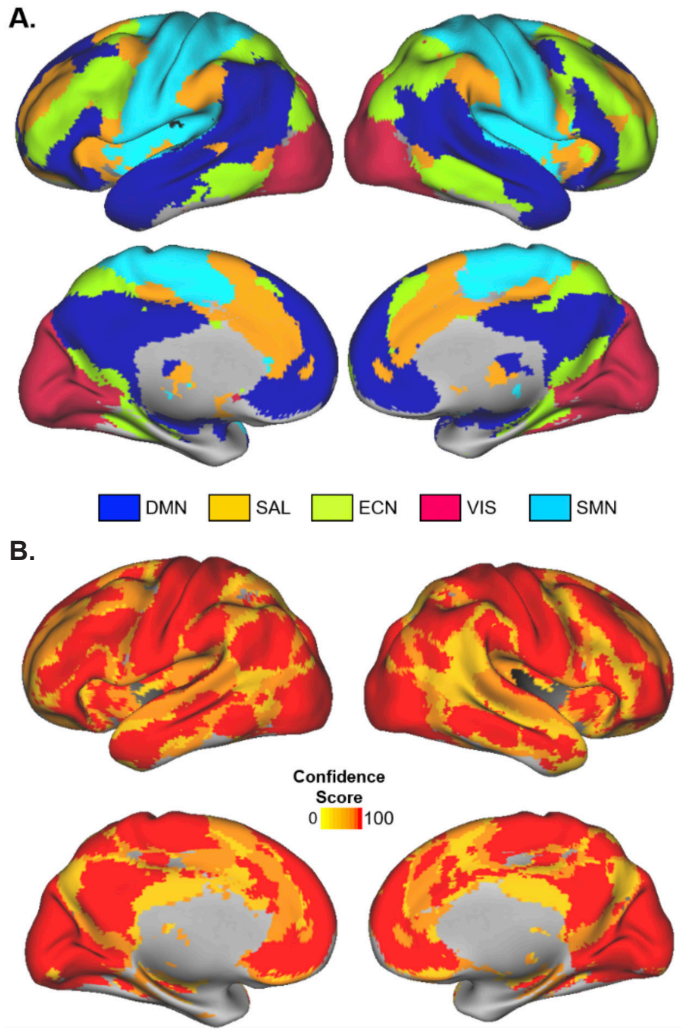

Figure 3. Atlas55+: Consensus brain atlas composed of the five major resting-state networks based on three cohorts of healthy individuals aged 55 years and above. (A) Spatial map of the RSNs. (B) Voxel-wise confidence map in Atlas55+. This measure quantifies the probability that a voxel in an Atlas55+ network is assigned to the same-label RSN in each of the three cohorts. DMN: Default mode network, SAL: Salience network, ECN: Executive control network, VIS: Visual network, SMN: Sensorimotor network.

Associations of sex and age with the spatial distribution of the major RSNs in Atlas55+

Sex: We did not find any significant differences between males and females on any of the spatial distribution of any RSN in the atlas.

Age: We found a negative regional association with age for each of the RSNs in the atlas (Figure 5, Supplementary Table S3). In detail, increasing age was associated with lower spatial integrity of: (i) both anterior and posterior medial regions in the DMN (Figure 5A), (ii) bilateral fronto-parietal regions in the ECN (Figure 5B), (iii) bilateral anterior insula and dorsal anterior cingulate cortex in the SAL (Figure 5C), (iv) bilateral superior temporal and postcentral gyri in the SMN (Figure 5D), and to a lesser degree (v) in

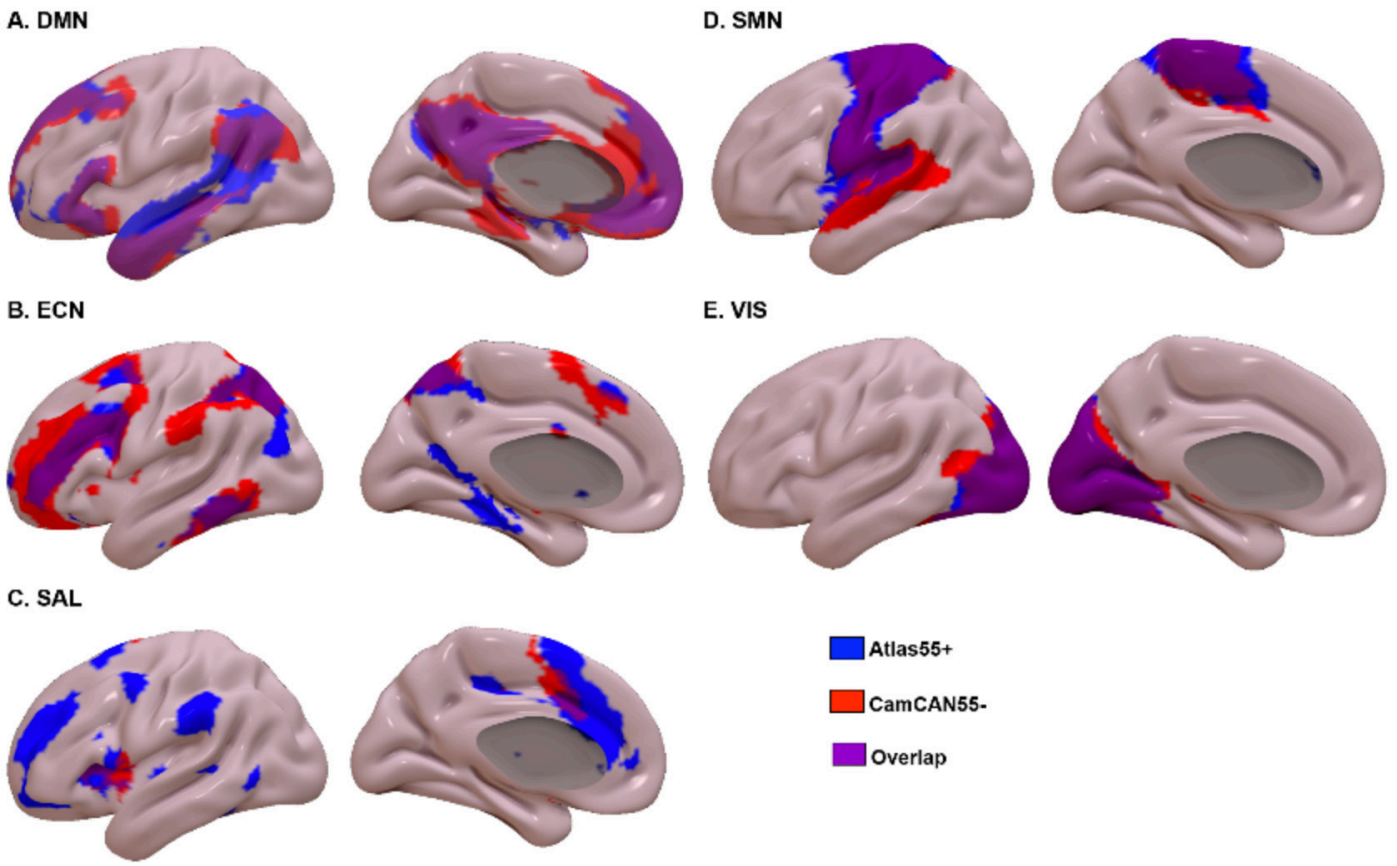

Figure 4. Spatial comparison of the major resting state networks between adults over the age of 55 years, as defined in Atlas55+, and younger adults (aged 18-54 years) from the CamCAN55- cohort.

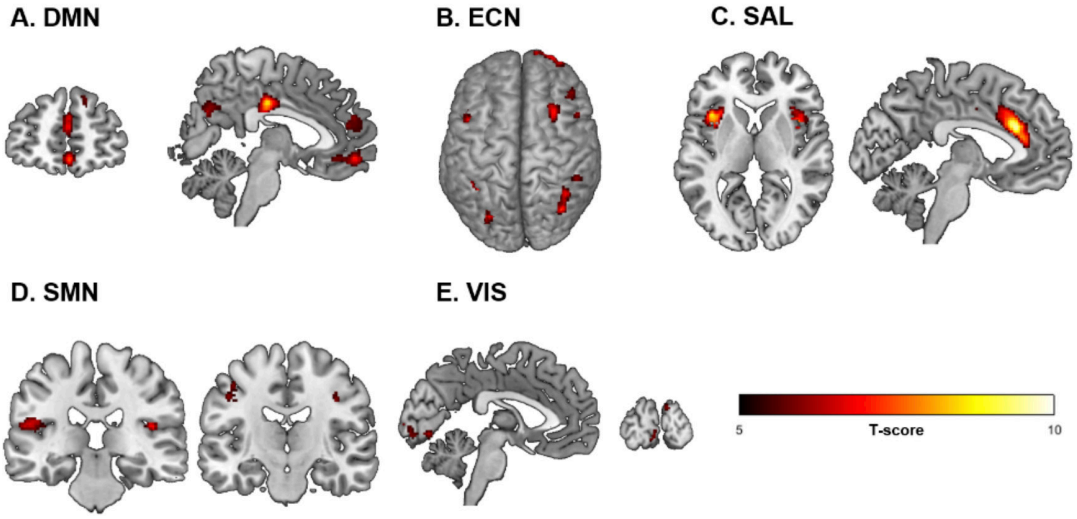

Figure 5. Clusters showing lower spatial integration with the rest of the RSN, with older age, across the three late-life cohorts. Details of the clusters are in Supplementary Table S3. Significance set up at $p<0.05$ (FWE correction at the voxel level).

the calcarine and lingual gyri of the VIS (Figure 5E).

In contrast, increasing age was associated with higher spatial integrity of cerebellar regions in both the DMN and the ECN (Supplementary Table S3). No other results were significant.

Discussion

This study investigated (a) the spatial definition of the major RSNs in healthy individuals in late adulthood using rs-fMRI data from three large independent cohorts of participants aged 55 and above and; (b) differences in the spatial definition of these RSNs with those in healthy mid-life adults. We found a high reproducibility of the spatial definition of the RSNs across the cohorts of older adults, but also significant differences when compared to the RSNs of mid-life adults. In response to these findings, we constructed Atlas55+, a robust brain functional atlas derived from rs-fMRI of 563 healthy adults between the ages of 55 and 95 years, in order to promote RSN reproducibility in future studies focusing on older populations. The age cut-off of 55 years may be considered arbitrary but there is currently no clear consensus on a specific age that distinguishes middle to late adulthood. In response, we followed the same age criterion as for the ADNI, which is a landmark initiative in North America to investigate brain organization in older populations (Jack et al., 2008; Petersen et al., 2010).

Despite different MRI scanner types, acquisition parameters, and sites, we demonstrated good

reproducibility of the spatial definition of the RSNs across the three aging cohorts. Regardless of the cohort, the regions with the highest spatial overlap between RSNs were localized in the medial prefrontal cortex, the precuneus, and the lateral parietal cortex, which have been described as brain hubs in young adults (Tomasi & Volkow, 2011; Zuo et al. 2012). These regions are thought to reflect an inherent feature of associative regions as these tend to participate in multiple networks (Yeo et al., 2014). While studies have reported a negative effect of aging on the strength of these regional hubs (Damoiseaux, 2017; Zhang et al., 2017), the current study suggests that the variability in their location remains relatively unaltered within older healthy populations.

Across the three late-life cohorts, we found that the most reproducible networks were the SMN and VIS networks. These networks are mostly covering primary cortices, which are known to have high structural-functional coherence (Luo et al., 2020a), low inter-individual variability in anatomical morphology (White et al., 1997) and in resting-state functional connectivity (Franco et al., 2013; Li et al., 2017; Mueller et al., 2013), and tend to preferentially participate in single networks in line with their circumscribed and specific functions (Yeo et al., 2014). In contrast, the SAL network showed the largest spatial differences across the three late-life cohorts. In studies of individuals below the age of 40 years, the spatial definition and role of the SAL network have been largely variable (Dosenbach et al., 2007; Doucet et al., 2019; Seeley et al., 2007; Shirer et al., 2012; Smith et al., 2009; Yeo et al., 2011) and this appears to be the case in older adults too.

In line with what we hypothesized, we found age-related alterations in the spatial composition of all five RSNs. The association of RSN spatial definition with age was examined in two different and complementary ways. First, by comparing RSNs between late- and mid-life adults and second by examining the effect of age within the older age-group by testing its association with RSN constitution in the RSNs defined by Atlas55+.

Comparison of mid- and late-life adults showed that the SMN and VIS showed the smallest differences, while the DMN, ECN and SAL showed the highest spatial reorganization. Several studies have consistently reported that the functional connectivity within networks supporting higher-order functions is more affected by age than that in networks supporting lower-order functions (Betzel et al., 2014; He et al., 2013; Mowinckel et al., 2012). Also, a recent study by Luo et al. (2020a) showed more extensive age-related changes in the structural-functional coherence of the associative cortex compared with that of the unimodal cortex. The posterior medial temporal regions - which are typically identified in the DMN in younger adults (Buckner et al., 2008; Buckner and DiNicola, 2019; Doucet et al., 2011) - were instead part of the ECN in the older adults. This finding is in agreement with the notion that cognitive aging involves reorganization of function, rather than a progressive loss of function (Andrews-Hanna et al., 2007; Reuter-Lorenz and Lustig, 2005; Yaple et al., 2019). This regional variability in the DMN and ECN is also supported by the model proposed by Turner and Spreng (2015) as the default to executive coupling hypothesis in aging (DECHA) that suggests a regional shift in the architecture of the DMN and ECN to support crystallized cognition in later life (Spreng et al., 2018). We also found large spatial differences in the SAL between the younger and older adults, with the younger adults showing a network restricted to the anterior insulas and anterior cingulate cortex only (Seeley et al. 2007). As discussed above, the origin of this large inter-individual variability is unclear. Future investigations focusing on the SAL are needed to determine whether the spatial differences may be related to analytical or true biological differences between samples.

Examination of the association of age with the functional integrity of the major RSNs in older adults, particularly in the major regions of the DMN, ECN and SAL. This finding was expected as the age range across all participants was 40 years. This was also consistent with prior neuroimaging studies that described an effect of aging on both brain structure and function in populations over age 50 (Betzel et al., 2014; Chan et al., 2014; Damoiseaux, 2017; Dima et al., 2020; Frangou et al., 2020; Luis et al., 2015; Luo et al., 2020b; Varangis et al., 2019a). The overall negative impact of age on each network largely confirms a reduction of functional cohesiveness of the major brain networks, particularly those supporting higher-order cognitive functions (Betzel et al., 2014; Damoiseaux et al., 2008; He et al., 2013; Mowinckel et al., 2012; Yaple et al., 2019). It is interesting to note that we also found a positive association of age in cerebellar regions in both the DMN and ECN, suggesting higher cerebellar-cortical integration in these two networks with older age. Zhang et al. (2017) found similar findings of increased cerebellar-neocortical functional connectivity with age in healthy participants between the age of 12 and 79 years. This higher cerebellar-neocortical integration has also been associated with successful higher-order cognitive activity in a healthy elderly population (Luis et al., 2015). Collectively, the findings reported in the current study underscore the importance of age-adapted brain functional atlases.

Moving forward, we propose Atlas55+ that has several advantages to study brain activity in late adulthood. To the best of our knowledge, Atlas55+ (a) is the only atlas based on rs-fMRI datasets from three independent cohorts including a total of 563 healthy participants above the age of 55 years; (b) is independent of variation in neuroimaging

parameters (site, MRI scanner and acquisition sequence); (c) is independent of sample composition.

While Atlas55+ offers a realistic option for standardizing the definition of RSNs for older adults, we acknowledge its limitations. First, the age cut-off of 55 years follows the criterion used in ADNI, but it can be viewed as arbitrary. Second, age-related changes in RSN configuration are likely to continue throughout late-life and these subtle changes may not be fully captured by Atlas55+. The option of creating brain functional atlases in older individuals to cover specific and smaller time periods (i.e., for every decade past the 55th year) is challenging at present as high-quality rs-fMRI datasets are scarce in older participants, particularly in advanced old age. The Human Connectome Project-Aging dataset may help achieve this goal when it will be fully released (https://www.humanconnectome.org/study/hcp-lifespan-aging). Third, we constructed Atlas55+ using a volumetric-based (ICA) rather than a surface-based approach. We previously demonstrated that MICCA provided reliable networks (Naveau et al., 2012), and the analytic approach does not significantly alter the reproducibility of the RSNs as long as they are derived from a sample of at least 100 individuals (Doucet et al., 2019), which is the case for each cohort analyzed in the current study. Therefore, it is unlikely that this choice strongly influenced the spatial definition of the RSNs. Fourth, we focused on the five major RSNs (DMN, ECN, SAL, SMN, VIS) as these are the most investigated and reproducible networks in the neuroimaging literature (Doucet et al., 2019; Elliott et al., 2019; van den Heuvel and Hulshoff Pol, 2010). As aging is associated with reduced brain modularity (Damoiseaux, 2017; Meunier et al., 2009; Varangis et al., 2019b), we cannot exclude the possibility that a different number of networks could have been identified using another type of clustering approach (Abou Elseoud et al., 2011). However, each of these five RSNs have been consistently identified in aging studies (Betzel et al., 2014; Damoiseaux et al., 2008; Mowinckel et al., 2012; Sala-Llonch et al., 2015; Varangis et al., 2019a), suggesting that their existence in older individuals is indisputable. For study designs that may focus on finer brain partitions in the elderly populations, the spatial maps of all the subnetworks are available upon request to the corresponding author.

Conclusion

We presented a quantitative comparison of the spatial composition of the major RSNs derived from healthy adults between the ages of 55 and 95 years old. We also identified the spatial distribution of age-related changes in RSN definition. Our results confirm the importance of age-appropriate brain functional atlases for studies investigating brain mechanisms related to aging. We propose that Atlas55+ can provide a reproducible template of the major RSNs for late adulthood, that is available upon request to the corresponding author.

Acknowledgments

GED is supported by the National Institute of Aging (R03AG064001) and the National Institute of General Medical Sciences (P20GM130447). LL is supported by a fellowship from the French Alternative Energies and Atomic Energy Commission (CEA). MJ is supported by a grant of the French government agency ANR (LABCOM Ginesislab, ANR 16-LCV2-0006-01). PT is supported by NIH grant U54 EB020403. SF is supported by the National Institute of Mental Health (R01MH113619).

Data and code availability

The datasets used in the current study are freely available or upon request (links provided in supplementary material). The RSNs extracted for each cohort and from Atlas55+ are available upon request to the corresponding author.

References

Abou Elseoud, A., Littow, H., Remes, J., Starck, T., Nikkinen, J., Nissila, J., Timonen, M., Tervonen, O., Kiviniemi, V., 2011. Group-ICA Model Order Highlights Patterns of Functional Brain Connectivity. Front Syst Neurosci 5, 37.

Andrews-Hanna, J.R., Snyder, A.Z., Vincent, J.L., Lustig, C., Head, D., Raichle, M.E., Buckner, R.L., 2007. Disruption of large-scale brain systems in advanced aging. Neuron 56, 924-935.

Beckmann, C.F., Mackay, C.E., Filippini, N., Smith, S.M., 2009. Group comparison of resting-state fMRI data using multi-subject ICA and dual regression. Organization of Human Brain Mapping.

Beckmann, C.F., Smith, S.M., 2004. Probabilistic independent component analysis for functional magnetic resonance imaging. IEEE Trans Med Imaging 23, 137-152.

Behzadi, Y., Restom, K., Liau, J., Liu, T.T., 2007. A component based noise correction method (CompCor) for BOLD and perfusion based fMRI. Neuroimage 37, 90-101.

Betzel, R.F., Byrge, L., He, Y., Goni, J., Zuo, X.N., Sporns, O., 2014. Changes in structu-

ral and functional connectivity among resting-state networks across the human lifespan. Neuroimage 102 Pt 2, 345-357.

Bijsterbosch, J.D., Woolrich, M.W., Glasser, M.F., Robinson, E.C., Beckmann, C.F., Van Essen, D.C., Harrison, S.J., Smith, S.M., 2018. The relationship between spatial configuration and functional connectivity of brain regions. Elife 7.

Buckner, R.L., Andrews-Hanna, J.R., Schacter, D.L., 2008. The brain's default network: anatomy, function, and relevance to disease. Ann N Y Acad Sci 1124, 1-38.

Buckner, R.L., DiNicola, L.M., 2019. The brain's default network: updated anatomy, physiology and evolving insights. Nat Rev Neurosci 20, 593-608.

Buckner, R.L., Krienen, F.M., Yeo, B.T., 2013. Opportunities and limitations of intrinsic functional connectivity MRI. Nat Neurosci 16, 832-837.

Buckner, R.L., Sepulcre, J., Talukdar, T., Krienen, F.M., Liu, H., Hedden, T., Andrews-Hanna, J.R., Sperling, R.A., Johnson, K.A., 2009. Cortical hubs revealed by intrinsic functional connectivity: mapping, assessment of stability, and relation to Alzheimer's disease. J Neurosci 29, 1860-1873.

Chan, M.Y., Park, D.C., Savalia, N.K., Petersen, S.E., Wig, G.S., 2014. Decreased segregation of brain systems across the healthy adult lifespan. Proc Natl Acad Sci U S A 111, E4997-5006.

Cordes, D., Haughton, V.M., Arfanakis, K., Carew, J.D., Turski, P.A., Moritz, C.H., Quigley, M.A., Meyerand, M.E., 2001. Frequencies contributing to functional connectivity in the cerebral cortex in "resting-state" data. AJNR Am J Neuroradiol 22, 1326-1333.

Damoiseaux, J.S., 2017. Effects of aging on functional and structural brain connectivity. Neuroimage 160, 32-40.

Damoiseaux, J.S., Beckmann, C.F., Arigita, E.J., Barkhof, F., Scheltens, P., Stam, C.J., Smith, S.M., Rombouts, S.A., 2008. Reduced resting-state brain activity in the "default network" in normal aging. Cereb Cortex 18, 1856-1864.

Damoiseaux, J.S., Rombouts, S.A., Barkhof, F., Scheltens, P., Stam, C.J., Smith, S.M., Beckmann, C.F., 2006. Consistent resting-state networks across healthy subjects. Proc Natl Acad Sci U S A 103, 13848-13853.

De Luca, M., Beckmann, C.F., De Stefano, N., Matthews, P.M., Smith, S.M., 2006. fMRI resting state networks define distinct modes of long-distance interactions in the human brain. Neuroimage 29, 1359-1367.

Dice, L.R., 1945. Measures of the amount of ecologic association between species. Ecology 26, 297-302.

Dima, D., Frangou, S., Group, E.-L.w., 2020. Subcortical Volume Trajectories across the Lifespan: Data from 18,605 healthy individuals aged 3-90 years. bioRxiv preprint.

Dong, D., Wang, Y., Chang, X., Luo, C., Yao, D., 2018. Dysfunction of Large-Scale Brain Networks in Schizophrenia: A Meta-analysis of Resting-State Functional Connectivity. Schizophr Bull 44, 168-181.

Dosenbach, N.U., Fair, D.A., Miezin, F.M., Cohen, A.L., Wenger, K.K., Dosenbach, R.A., Fox, M.D., Snyder, A.Z., Vincent, J.L., Raichle, M.E., Schlaggar, B.L., Petersen, S.E., 2007. Distinct brain networks for adaptive and stable task control in humans. Proc Natl Acad Sci U S A 104, 11073-11078.

Doucet, G., Naveau, M., Petit, L., Delcroix, N., Zago, L., Crivello, F., Jobard, G., Tzourio-Mazoyer, N., Mazoyer, B., Mellet, E., Joliot, M., 2011. Brain activity at rest: a multiscale hierarchical functional organization. J Neurophysiol 105, 2753-2763.

Doucet, G., Naveau, M., Petit, L., Zago, L., Crivello, F., Jobard, G., Delcroix, N., Mellet, E., Tzourio-Mazoyer, N., Mazoyer, B., Joliot, M., 2012. Patterns of hemodynamic low-frequency oscillations in the brain are modulated by the nature of free thought during rest. Neuroimage 59, 3194-3200.

Doucet, G.E., Bassett, D.S., Yao, N., Glahn, D.C., Frangou, S., 2017. The Role of Intrinsic Brain Functional Connectivity in Vulnerability and Resilience to Bipolar Disorder. Am J Psychiatry 174, 1214-1222.

Doucet, G.E., Lee, W.H., Frangou, S., 2019. Evaluation of the spatial variability in the major resting-state networks across human brain functional atlases. Hum Brain Mapp 40, 4577-4587.

Elliott, M.L., Knodt, A.R., Cooke, M., Kim, M.J., Melzer, T.R., Keenan, R., Ireland, D., Ramrakha, S., Poulton, R., Caspi, A., Moffitt, T.E., Hariri, A.R., 2019. General functional connectivity: Shared features of resting-state and task fMRI drive reliable and heritable individual differences in functional brain networks. Neuroimage 189, 516-532.

Feltz, C.J., Miller, G.E., 1996. An asymptotic test for the equality of coefficients of variation from k populations. Stat Med 15, 646-658.

Fox, M.D., Snyder, A.Z., Vincent, J.L., Corbetta, M., Van Essen, D.C., Raichle, M.E., 2005.

The human brain is intrinsically organized into dynamic, anticorrelated functional networks. Proc Natl Acad Sci U S A 102, 9673-9678.

Franco, A.R., Mannell, M.V., Calhoun, V.D., Mayer, A.R., 2013. Impact of analysis methods on the reproducibility and reliability of resting-state networks. Brain Connect 3, 363-374.

Frangou, S., Dima, D., group, E.-l.w., 2020. Cortical Thickness Trajectories across the Lifespan: Data from 17,075 healthy individuals aged 3-90 years. bioRxiv preprint.

Friston, K.J., Williams, S., Howard, R., Frackowiak, R.S., Turner, R., 1996. Movement-related effects in fMRI time-series. Magn Reson Med 35, 346-355.

Greicius, M.D., Supekar, K., Menon, V., Dougherty, R.F., 2009. Resting-state functional connectivity reflects structural connectivity in the default mode network. Cereb Cortex 19, 72-78.

He, X., Qin, W., Liu, Y., Zhang, X., Duan, Y., Song, J., Li, K., Jiang, T., Yu, C., 2013. Age-related decrease in functional connectivity of the right fronto-insular cortex with the central executive and default-mode networks in adults from young to middle age. Neurosci Lett 544, 74-79.

Himberg, J., Hyvarinen, A., Esposito, F., 2004. Validating the independent components of neuroimaging time series via clustering and visualization. Neuroimage 22, 1214-1222.

Hyvarinen, A., 1999. Fast and robust fixed-point algorithms for independent component analysis. IEEE Trans Neural Netw 10, 626-634.

Jack, C.R., Jr., Bernstein, M.A., Fox, N.C., Thompson, P., Alexander, G., Harvey, D., Borowski, B., Britson, P.J., J, L.W., Ward, C., Dale, A.M., Felmlee, J.P., Gunter, J.L., Hill, D.L., Killiany, R., Schuff, N., Fox-Bosetti, S., Lin, C., Studholme, C., DeCarli, C.S., Krueger, G., Ward, H.A., Metzger, G.J., Scott, K.T., Mallozzi, R., Blezek, D., Levy, J., Debbins, J.P., Fleisher, A.S., Albert, M., Green, R., Bartzokis, G., Glover, G., Mugler, J., Weiner, M.W., 2008. The Alzheimer's Disease Neuroimaging Initiative (ADNI): MRI methods. J Magn Reson Imaging 27, 685-691.

Kiviniemi, V., Starck, T., Remes, J., Long, X., Nikkinen, J., Haapea, M., Veijola, J., Moilanen, I., Isohanni, M., Zang, Y.F., Tervonen, O., 2009. Functional segmentation of the brain cortex using high model order group PICA. Hum Brain Mapp 30, 3865-3886.

Labache, L., Joliot, M., Saracco, J., 2020. Study of the inter-individual variability of intrinsic connectivity data: detection of unstable networks and sub-populations in a three-dimensional table. arXiv preprint arXiv:2004.05033.

Li, R., Yin, S., Zhu, X., Ren, W., Yu, J., Wang, P., Zheng, Z., Niu, Y.N., Huang, X., Li, J., 2017. Linking Inter-Individual Variability in Functional Brain Connectivity to Cognitive Ability in Elderly Individuals. Front Aging Neurosci 9, 385.

Luis, E.O., Arrondo, G., Vidorreta, M., Martinez, M., Loayza, F., Fernandez-Seara, M.A., Pastor, M.A., 2015. Successful Working Memory Processes and Cerebellum in an Elderly Sample: A Neuropsychological and fMRI Study. PLoS One 10, e0131536.

Luo, N., Sui, J., Abrol, A., Chen, J., Turner, J.A., Damaraju, E., Fu, Z., Fan, L., Lin, D., Zhuo, C., Xu, Y., Glahn, D.C., Rodrigue, A.L., Banich, M.T., Pearlson, G.D., Calhoun, V.D., 2020a. Structural Brain Architectures Match Intrinsic Functional Networks and Vary across Domains: A Study from 15 000+ Individuals. Cereb Cortex.

Luo, N., Sui, J., Abrol, A., Lin, D., Chen, J., Vergara, V.M., Fu, Z., Du, Y., Damaraju, E., Xu, Y., Turner, J.A., Calhoun, V.D., 2020b. Age-related structural and functional variations in 5,967 individuals across the adult lifespan. Hum Brain Mapp 41, 1725-1737.

Meunier, D., Achard, S., Morcom, A., Bullmore, E., 2009. Age-related changes in modular organization of human brain functional networks. Neuroimage 44, 715-723.

Minka, T., 2000. Automatic choice of dimensionality for PCA. In: MIT (Ed.), Media Laboratory Perceptual Computing Section Technical Report.

Mowinckel, A.M., Espeseth, T., Westlye, L.T., 2012. Network-specific effects of age and in-scanner subject motion: a resting-state fMRI study of 238 healthy adults. Neuroimage 63, 1364-1373.

Mueller, S., Wang, D., Fox, M.D., Yeo, B.T., Sepulcre, J., Sabuncu, M.R., Shafee, R., Lu, J., Liu, H., 2013. Individual variability in functional connectivity architecture of the human brain. Neuron 77, 586-595.

Naveau, M., Doucet, G., Delcroix, N., Petit, L., Zago, L., Crivello, F., Jobard, G., Mellet, E., Tzourio-Mazoyer, N., Mazoyer, B., Joliot, M., 2012. A novel group ICA approach based on multi-scale individual component clustering. Application to a large sample of fMRI data. Neuroinformatics 10, 269-285.

Nickerson, L.D., Smith, S.M., Ongur, D., Beckmann, C.F., 2017. Using Dual Regression to Investigate Network Shape and Amplitude in Functional Connectivity Analyses. Front Neurosci 11, 115.

Patel, A.X., Kundu, P., Rubinov, M., Jones, P.S., Vertes, P.E., Ersche, K.D., Suckling, J., Bullmore, E.T., 2014. A wavelet method for modeling and despiking motion artifacts from resting-state fMRI time series. Neuroimage 95, 287-304.

Petersen, R.C., Aisen, P.S., Beckett, L.A., Donohue, M.C., Gamst, A.C., Harvey, D.J., Jack, C.R., Jr., Jagust, W.J., Shaw, L.M., Toga, A.W., Trojanowski, J.Q., Weiner, M.W., 2010. Alzheimer's Disease Neuroimaging Initiative (ADNI): clinical characterization. Neurology 74, 201-209.

Power, J.D., Barnes, K.A., Snyder, A.Z., Schlaggar, B.L., Petersen, S.E., 2012. Spurious but systematic correlations in functional connectivity MRI networks arise from subject motion. Neuroimage 59, 2142-2154.

Reuter-Lorenz, P.A., Lustig, C., 2005. Brain aging: reorganizing discoveries about the aging mind. Curr Opin Neurobiol 15, 245-251.

Sala-Llonch, R., Bartres-Faz, D., Junque, C., 2015. Reorganization of brain networks in aging: a review of functional connectivity studies. Front Psychol 6, 663.

Salman, M.S., Du, Y., Lin, D., Fu, Z., Fedorov, A., Damaraju, E., Sui, J., Chen, J., Mayer, A.R., Posse, S., Mathalon, D.H., Ford, J.M., Van Erp, T., Calhoun, V.D., 2019. Group ICA for identifying biomarkers in schizophrenia: 'Adaptive' networks via spatially constrained ICA show more sensitivity to group differences than spatio-temporal regression. Neuroimage Clin 22, 101747.

Seeley, W.W., Menon, V., Schatzberg, A.F., Keller, J., Glover, G.H., Kenna, H., Reiss, A.L., Greicius, M.D., 2007. Dissociable intrinsic connectivity networks for salience processing and executive control. J Neurosci 27, 2349-2356.

Sha, Z., Wager, T.D., Mechelli, A., He, Y., 2019. Common Dysfunction of Large-Scale Neurocognitive Networks Across Psychiatric Disorders. Biol Psychiatry 85, 379-388.

Shafto, M.A., Tyler, L.K., Dixon, M., Taylor, J.R., Rowe, J.B., Cusack, R., Calder, A.J., Marslen-Wilson, W.D., Duncan, J., Dalgleish, T., Henson, R.N., Brayne, C., Matthews, F.E., Cam, C.A.N., 2014. The Cambridge Centre for Ageing and Neuroscience (Cam-CAN) study protocol: a cross-sectional, lifespan, multidisciplinary examination of healthy cognitive ageing. BMC Neurol 14, 204.

Shirer, W.R., Ryali, S., Rykhlevskaia, E., Menon, V., Greicius, M.D., 2012. Decoding subject-driven cognitive states with whole-brain connectivity patterns. Cereb Cortex 22, 158-165.

Smith, S.M., Fox, P.T., Miller, K.L., Glahn, D.C., Fox, P.M., Mackay, C.E., Filippini, N., Watkins, K.E., Toro, R., Laird, A.R., Beckmann, C.F., 2009. Correspondence of the brain's functional architecture during activation and rest. Proc Natl Acad Sci U S A 106, 13040-13045.

Smith, S.M., Jenkinson, M., Woolrich, M.W., Beckmann, C.F., Behrens, T.E., Johansen-Berg, H., Bannister, P.R., De Luca, M., Drobnjak, I., Flitney, D.E., Niazy, R.K., Saunders, J., Vickers, J., Zhang, Y., De Stefano, N., Brady, J.M., Matthews, P.M., 2004. Advances in functional and structural MR image analysis and implementation as FSL. Neuroimage 23 Suppl 1, S208-219.

Smith, S.M., Nichols, T.E., Vidaurre, D., Winkler, A.M., Behrens, T.E., Glasser, M.F., Ugurbil, K., Barch, D.M., Van Essen, D.C., Miller, K.L., 2015. A positive-negative mode of population covariation links brain connectivity, demographics and behavior. Nat Neurosci 18, 1565-1567.

Spreng, R.N., Lockrow, A.W., DuPre, E., Setton, R., Spreng, K.A.P., Turner, G.R., 2018. Semanticized autobiographical memory and the default - executive coupling hypothesis of aging. Neuropsychologia 110, 37-43.

Taylor, J.R., Williams, N., Cusack, R., Auer, T., Shafto, M.A., Dixon, M., Tyler, L.K., Cam, C., Henson, R.N., 2017. The Cambridge Centre for Ageing and Neuroscience (Cam-CAN) data repository: Structural and functional MRI, MEG, and cognitive data from a cross-sectional adult lifespan sample. Neuroimage 144, 262-269.

Toosy, A.T., Ciccarelli, O., Parker, G.J., Wheeler-Kingshott, C.A., Miller, D.H., Thompson, A.J., 2004. Characterizing function-structure relationships in the human visual system with functional MRI and diffusion tensor imaging. Neuroimage 21, 1452-1463.

Tracy, J.I., Doucet, G.E., 2015. Resting-state functional connectivity in epilepsy: growing relevance for clinical decision making. Curr Opin Neurol 28, 158-165.

Turner, G.R., Spreng, R.N., 2015. Prefrontal Engagement and Reduced Default Network Suppression Co-occur and Are Dynamically Coupled in Older Adults: The Default-Executive Coupling Hypothesis of Aging. J Cogn Neurosci 27, 2462-2476.

van den Heuvel, M.P., Hulshoff Pol, H.E., 2010. Exploring the brain network: a review on resting-state fMRI functional connectivity. Eur Neuropsychopharmacol 20, 519-534.

van den Heuvel, M.P., Mandl, R.C., Kahn, R.S., Hulshoff Pol, H.E., 2009. Functionally linked resting-state networks reflect the underlying structural connectivity architecture of the

human brain. Hum Brain Mapp 30, 3127-3141.

Varangis, E., Habeck, C.G., Razlighi, Q.R., Stern, Y., 2019a. The Effect of Aging on Resting State Connectivity of Predefined Networks in the Brain. Front Aging Neurosci 11, 234.

Varangis, E., Razlighi, Q., Habeck, C.G., Fisher, Z., Stern, Y., 2019b. Between-network Functional Connectivity Is Modified by Age and Cognitive Task Domain. J Cogn Neurosci 31, 607-622.

Wei, D., Zhuang, K., Chen, Q., Yang, W., Liu, W., Wang, K., Sun, J., Qui, J., 2018. Structural and functional MRI from a cross-sectional Southwest University Adult lifespan Dataset (SALD). bioRxiv.

White, L.E., Andrews, T.J., Hulette, C., Richards, A., Groelle, M., Paydarfar, J., Purves, D., 1997. Structure of the human sensorimotor system. I: Morphology and cytoarchitecture of the central sulcus. Cereb Cortex 7, 18-30.

Yan, C.G., Wang, X.D., Zuo, X.N., Zang, Y.F., 2016. DPABI: Data Processing & Analysis for (Resting-State) Brain Imaging. Neuroinformatics 14, 339-351.

Yaple, Z.A., Stevens, W.D., Arsalidou, M., 2019. Meta-analyses of the n-back working memory task: fMRI evidence of age-related changes in prefrontal cortex involvement across the adult lifespan. Neuroimage 196, 16-31.

Yeo, B.T., Krienen, F.M., Chee, M.W., Buckner, R.L., 2014. Estimates of segregation and overlap of functional connectivity networks in the human cerebral cortex. Neuroimage 88, 212-227.

Yeo, B.T., Krienen, F.M., Sepulcre, J., Sabuncu, M.R., Lashkari, D., Hollinshead, M., Roffman, J.L., Smoller, J.W., Zollei, L., Polimeni, J.R., Fischl, B., Liu, H., Buckner, R.L., 2011. The organization of the human cerebral cortex estimated by intrinsic functional connectivity. J Neurophysiol 106, 1125-1165.

Zalesky, A., Fornito, A., Harding, I.H., Cocchi, L., Yucel, M., Pantelis, C., Bullmore, E.T., 2010. Whole-brain anatomical networks: does the choice of nodes matter? Neuroimage 50, 970-983.

Zhang, H., Lee, A., Qiu, A., 2017. A posterior-to-anterior shift of brain functional dynamics in aging. Brain Struct Funct 222, 3665-3676.